Available online at www.sciencedirect.com

ScienceDirect

Mendeleev Commun., 2018, **28**, 556–558

Mendeleev Communications

Polyacrylonitrile molecular weight effect on the structural and magnetic properties of metal–carbon nanomaterial

Mikhail N. Efimov,*[a] Andrey A. Vasilev,[a,b] Elena V. Chernikova,[a,c] Roman V. Toms,[d] Dmitriy G. Muratov,[a,b] Galina V. Pankina,[c] Petr A. Chernavskii[c] and Galina P. Karpacheva[a]

[a] *A. V. Topchiev Institute of Petrochemical Synthesis, Russian Academy of Sciences, 119991 Moscow, Russian Federation. E-mail: efimov@ips.ac.ru*
[b] *National University of Science and Technology 'MISiS', 119049 Moscow, Russian Federation*
[c] *Department of Chemistry, M. V. Lomonosov Moscow State University, 119991 Moscow, Russian Federation*
[d] *Institute of Fine Chemical Technologies, Moscow Technological University, 119454 Moscow, Russian Federation*

DOI: 10.1016/j.mencom.2018.09.037

The influence of the molecular-weight parameters of the polymer on the functional properties of metal–carbon nanomaterials (MCN) was revealed for the first time. A difference in the phase composition of iron-containing nanoparticles was established employing high and low molecular weight polyacrylonitrile, which determines the magnetic characteristics of the MCN.

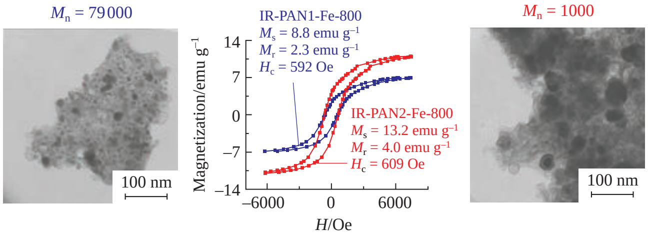

Metallic nanoparticles immobilized on various supports attract the attention of researchers due to the multifunctional features of the resulting 'support–nanoparticles' systems.[1,2] The properties of these materials are mainly caused by the nature of the introduced metals or their combination. Supports can also play an important role.[3–5] Carbon and its various forms are well known as one of the most promising types of support.[6] The advantages of carbon supports include their chemical resistance to aggressive media, thermal stability, electrochemical and catalytic properties, a large specific surface area, and a wide variety of carbonaceous precursors.[7,8]

Two strategies for the preparation of metal–carbon nanomaterials (MCN) are well known: deposition of nanoparticles on the prepared carbon support obtained *via* carbonaceous precursor heat treatment and mixing of a carbonaceous precursor with salts or formed metallic nanoparticles followed by annealing. Here, we report on the method for MCN preparation *via* IR radiation mediated pyrolysis of a precursor based on polyacrylonitrile (PAN) and iron acetylacetonate.

The present study was aimed to determine an effect of the molecular weight of polymer used as the carbonaceous precursor for the support on the structural and, consequently, functional properties of synthesized nanomaterials, *i.e.* to reveal the possibility of regulating the phase composition, structural and functional characteristics by varying one of the support parameters.[†]

The synthetic method applied can significantly shorten the preparation time of MCN down to several minutes due to both the simultaneous carbon support and metallic nanoparticles formation and heat treatment by IR irradiation that stimulates the chemical transformations of PAN.[9,10]

The shape and size of iron-containing particles, the carbon structure formed during the polymer pyrolysis, and the interaction of the polymer matrix with iron were revealed by TEM.[‡] According to Figure 1, the most of particles possess a shape close to spherical. TEM images analysis of the distribution of iron-containing nanoparticle sizes showed that in IR-PAN1-Fe-800 sample, the average size is smaller than in the nanomaterial based on PAN2 (8 and 23 nm, respectively). In addition, TEM images display ordered carbon structures and carbon shells formed due to the interaction between carbon atoms and iron, which is capable of structuring and graphitizing carbon with the subsequent carbon shell formation.[11] These carbon shells are well recognizable around larger nanoparticles. As demonstrated in micrographs, a large amount of circular or ring-like ordered graphite carbon species were observed along with amorphous carbon.

The carbon phase evolution and the formation of iron-containing nanoparticles in the carbonized polymer was detected by XRD. Thus, the diffraction peaks of γ-Fe are present in addition to the reflections of iron carbides in the XRD patterns of IR-PAN1-Fe-800 and IR-PAN2-Fe-800 (Figure 2).[‡] The carbon phase diffraction

---

[†] High-molecular-weight PAN (PAN1) was obtained by radical polymerization in an aqueous medium in the presence of ammonium persulfate and sodium dithionite at 60 °C (M_n = 79 000, M_w/M_n = 3.54). Oligomeric PAN (PAN2) was synthesized by radical polymerization *via* reversible chain transfer in a solution of *N*-methylmorpholine oxide in the presence of AIBN and dibenzyl trithiocarbonate at 80 °C (M_n = 1000, M_w/M_n = = 1.35). MCN based on the iron-containig nanoparticles and carbon support were synthesized by pyrolysis of a film from a co-solution of the polymer and iron acetylacetonate under IR irradiation similar to the described procedure.[9] A co-solution of PAN and $Fe(C_5H_7O_2)_3$ (Acros Organics, >99%) in DMF (Fisher Chemical, synthesis grade) was dried at 70 °C. The weight ratio of carbon to iron was 10 : 1. The obtained film was ground and subjected to preliminary IR heating at 200 °C in air, followed by IR treatment under an inert atmosphere at 800 °C.

[‡] Transmission electron microscopy (TEM) images were obtained using a LEO912 AB OMEGA transmission electron microscope. TEM micrographs were used to calculate the distribution of nanoparticle sizes *via* MicrAn program. Powder X-ray diffraction (XRD) analysis was performed on a Difray diffractometer with Bragg–Brentano focusing, using CrKα radiation.

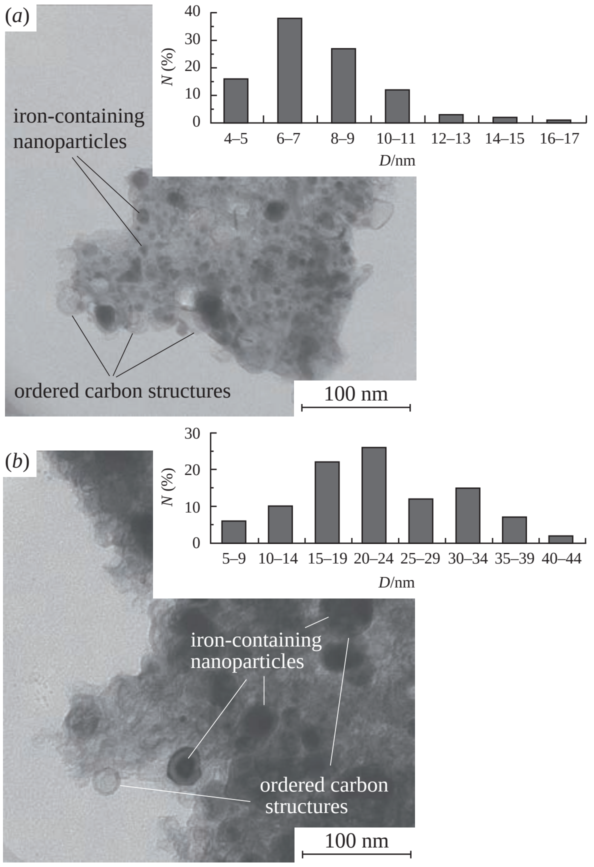

Figure 1 TEM images of (*a*) IR-PAN1-Fe-800 and (*b*) IR-PAN2-Fe-800. The insets show iron-containing nanoparticle size distribution for the corresponding samples.

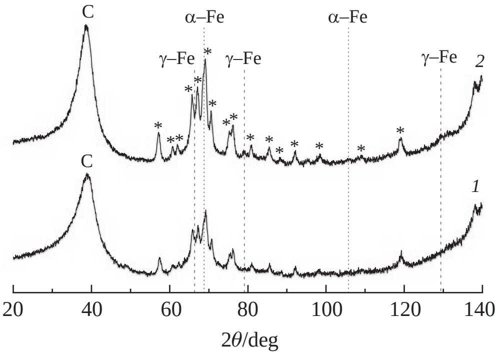

Figure 2 XRD patterns of (*1*) IR-PAN1-Fe-800 and (*2*) IR-PAN2-Fe-800. The Fe$_3$C phase is denoted by asterisks.

peaks for PAN1 and PAN2 samples are similar, which can be explained by the formation of carbon shells around iron-containing nanoparticles.

Note that XRD analysis data is in good agreement with the TEM data. Considering a lower yield of PAN2-based nanomaterial, it is supposed that the low molecular weight polymer was pyrolyzed more easily to give huge amount of decomposition products, which can interact with iron resulting in larger ordered carbon shells formation.

Since the iron carbide reflections are located in the region of the most intensive α- and γ-Fe phases diffraction peaks, the Mössbauer spectroscopy method was employed to refine the phase composition and iron distribution in the phases (Table 1). Figure 3(*a*)[§]

Table 1 Mössbauer spectra parameters of the IR-PAN-Fe samples.

Sample	Label[a]	δ[b]/mm s^{-1}	Δ[c]/mm s^{-1}	H[d]/kOe	S[e] (%)	Phase
IR-PAN1-Fe	S1	–0.02	–0.02	331	3.6	α-Fe
	S2	0.18	0.02	208	66.2	Fe$_3$C
	S3	0.17	–0.05	194	13.6	Fe$_3$C[f]
	S4	0.51	–0.03	82	10.0	Fe$_3$C[f]
	M	–0.10	0.00	0	6.6	γ-Fe
IR-PAN2-Fe	S1	–0.02	0.02	333	6.0	α-Fe
	S2	0.18	0.02	208	87.8	Fe$_3$C
	M	–0.08	0.00	0	6.2	γ-Fe

[a]Labels of spectral components given in Figure 3(*a*). [b]Isomer shift relative to α-Fe. [c]Quadrupole splitting. [d]Magnetic field value at the ^{57}Fe nucleus. [e]Component area. [f]Sextets from disordered phases in Fe$_{3-x}$C$_{1+x}$ composition.

demonstrates the Mössbauer spectra of the IR-PAN1-Fe-800 and IR-PAN2-Fe-800 samples. In addition to the sextets (δ = = 0.18 mm s^{-1}, Δ = 0.02 mm s^{-1}, H = 208 kOe) belonging to the iron carbide ferromagnetic phases (Fe$_3$C), a monoline (δ = = –0.1 mm s^{-1}, Δ = 0, and H = 0 kOe) corresponding to the γ-Fe phase (austenite) and also the α-Fe sextet phase (δ = = –0.02 mm s^{-1}, Δ = 0.02, and H = 332 kOe) were observed. The values of areas under the resonance lines (6 and 6.5 rel%) indicate that the content of γ-Fe is very similar in the two samples regardless of the molecular weight. However, the α-Fe content is twice higher in IR-PAN2-Fe-800, while the phases of slightly ordered iron carbide with the composition of Fe$_{3-x}$C$_{1+x}$ (the magnetic field on ^{57}Fe nuclei is reduced from 208 down to 82 kOe) are observed in IR-PAN1-Fe-800.

The investigation of magnetic properties [Figure 3(*b*)][§] has showed that the samples synthesized at 800 °C are characterized by magnetization hysteresis loops. The saturated magnetization of IR-PAN2-Fe-800 (M_s = 13.2 emu g^{-1}) is much higher as compared to IR-PAN1-Fe-800 (M_s = 8.8 emu g^{-1}) sample, which is in agreement with the data of Mössbauer spectroscopy and XRD. These results are explained by both the ordered structure

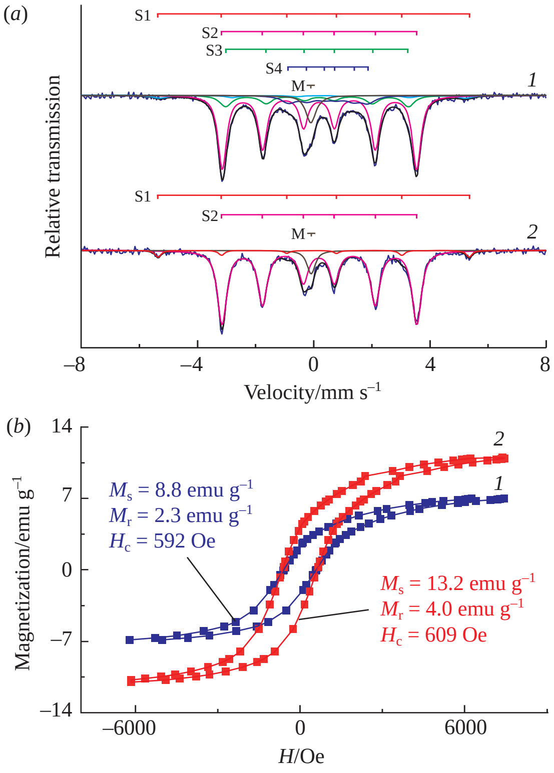

Figure 3 (*a*) Mössbauer spectra of (*1*) IR-PAN1-Fe-800 and (*2*) IR-PAN2-Fe-800 samples with marked components (see Table 1) and (*b*) magnetization curves.

[§] The Mössbauer spectra were recorded on a Es-1104 Em spectrometer equipped with a ^{57}Co γ-radiation source at room temperature. Magnetization curves were obtained on a vibrating magnetometer at room temperature.[12]

of Fe_3C carbide and the increased content of the α-Fe magnetic phase in IR-PAN2-Fe-800 sample. The coercive force values of both MCN are very similar (592 and 609 Oe) and caused by the properties of iron carbide as the main metal-containing phase. The growth of residual magnetization can also be explained by both the larger size and the more ordered structure of nanoparticles of ferromagnetic phases.

In summary, PAN-based MCN with similar structures have been prepared despite the huge difference in the molecular weight of the polymers. It has for the first time been demonstrated that the variation of the characteristics of a polymer, as a carbon precursor, allows one to control the phase composition of the formed iron-containing nanoparticles and, as a consequence, the functional features (*e.g.*, magnetic properties) of the obtained MCN. It has been revealed that the polymer with a larger molecular weight allows one to obtain iron-containing nanoparticles of smaller size.

This work was carried out within the State Program at A. V. Topchiev Institute of Petrochemical Synthesis of the Russian Academy of Sciences.

References

1 *Multifunctional Nanocomposites for Energy and Environmental Applications*, eds. Z. Guo, Y. Chen and N. L. Lu, Wiley-VCH, Weinheim, 2018.
2 A. A. Efimova, T. E. Grokhovskaya and A. V. Efimov, *Mendeleev Commun.*, 2017, **27**, 315.
3 D. Pandey and G. Deo, *J. Ind. Eng. Chem.*, 2016, **33**, 99.
4 T. Fu, Y. Jiang, J. Lv and Z. Li, *Fuel Process. Technol.*, 2013, **110**, 141.
5 A. Volynkin, M. Rønning and E. A. Blekkan, *Top. Catal.*, 2015, **58**, 854.
6 E. Lam and J. H. T. Luong, *ACS Catal.*, 2014, **4**, 3393.
7 E. Auer, A. Freund, J. Pietsch and T. Tacke, *Appl. Catal. A*, 1998, **173**, 259.
8 P. Trogadas, T. F. Fuller and P. Strasser, *Carbon*, 2014, **75**, 5.
9 M. V. Kulikova, L. M. Zemtsov, S. A. Sagitov, M. N. Efimov, A. Yu. Krylova, G. P. Karpacheva and S. N. Khadzhiev, *Solid Fuel Chem.*, 2014, **48**, 105 (*Khim. Tverd. Topliva*, 2014, no. 2, 32).
10 E. V. Chernikova, Z. A. Poteryaeva, A. V. Shlyakhtin, N. I. Prokopov, A. Yu. Gerval'd, A. Yu. Nikolaev, V. R. Duflot, E. A. Dubova, Yu. V. Kostina, A. S. Rodionov, M. N. Efimov, A. S. Cherevan' and G. N. Bondarenko, *Polym. Sci., Ser. B*, 2013, **55**, 1 (*Vysokomol. Soedin., Ser. B*, 2013, **55**, 66).
11 H. Marsh, D. Crawford and D. W. Taylor, *Carbon*, 1983, **21**, 81.
12 P. A. Chernavskii, A. Y. Khodakov, G. V. Pankina, J.-S. Girardon and E. Quinet, *Appl. Catal.*, 2006, **306**, 108.

Received: 9th April 2018; Com. 18/5533